CORROSION BEHAVIOR OF MILD STEEL IN HIGH pH AQUEOUS MEDIA

Anna C. Fraker and Jonice S. Harris

U.S. DEPARTMENT OF COMMERCE
National Institute of Standards and Technology
Institute for Materials Science and Engineering
Metallurgy Division
Gaithersburg, MD 20899

NIST

CORROSION BEHAVIOR OF MILD STEEL IN HIGH pH AQUEOUS MEDIA

Anna C. Fraker and
Jonice S. Harris

U.S. DEPARTMENT OF COMMERCE
National Institute of Standards
and Technology
Institute for Materials Science
and Engineering
Metallurgy Division
Gaithersburg, MD 20899

CORROSION BEHAVIOR OF MILD STEEL IN HIGH pH AQUEOUS MEDIA

INTRODUCTION

Purpose

This work was conducted to study the corrosion behavior and localized corrosion susceptibility of American Society for Testing and Materials (ASTM) A-27 steel in simulated ground water at a pH of 9.75 and a temperature of 95°C. These studies were conducted as part of a program to evaluate materials for use in long term nuclear waste storage.

The test conditions used in the present study typify those of a basalt repository in the state of Washington and simulated test solution representative of that area, but selected aspects of the results are applicable to low alloy steels in other environments containing the same ions. Some additional tests were conducted in simulated well water, typifying water which is found near the nuclear waste storage site in tuffaceous rock in Nye County, Nevada.

Background

Various aspects of pitting have been discussed previously [1,2,3]. Studies[4] of A-27 and similar steel in the Grande Ronde 4 water environment indicated that pits were occasionally found after testing but stated that pitting would not develop in repository conditions· A passive region in the anodic polarization curves was observed in this study[4] at temperatures of 150°C and 200°C and a smaller passive region was observed after one week's exposure at 100°C. Other investigations[5] included A-27 steel, and obtained a corrosion rate of 0.21 mils per year (mpy)· One mpy is equal to 0.001 in. per year or 0.0254 mm per year. This corrosion rate was determined after approximately two years exposure in anoxic brine at 150°C. This corrosion rate from the anoxic brine was doubled for specimens exposed in oxic brine and was a little more than tripled for specimens when gamma radiation was added to the environment. Significant quantities of magnesium ions caused a thirty fold increase in these corrosion rates. Other reports on corrosion of mild steel in aqueous media indicated uneven attack over the specimen surface but did not indicate pitting attack[5].

Pitting[1,2] is the result of local breakdown of the passive film at sites of inclusions, defects, cracks, etc. If rapid repassivation does not occur, chemical conditions within the pit cause the pit to be anodic (actively corroding) to the rest of the metal surface (cathode) and the pits will grow. The pitting potential[2] at which localized breakdown of the passive film occurs is more noble than the corrosion potential, and the protection potential, below which pitting will not occur and existing pits will not propagate, also is more noble than the corrosion potential.

If the protection potential is at the corrosion potential, pitting will occur after an incubation period. If the pitting potential is the same as the corrosion potential, pitting will occur immediately.

There are other circumstances in which pitting or localized attack can occur but deep pits do not result. For example, pitting may occur at a potential where the metal is undergoing active corrosion or at the point where the metal changes from active corrosion to the passive state[3], and in these cases, general corrosion occurs and deep pits do not develop. Pitting at cathodic potentials has been reported for austenitic stainless steel[6] and for passivated iron[7,8]. The latter work concluded that the pitting potential was a mixed potential with cathodic dissolution as well as anodic dissolution occurring. Other work indicated that reactions in local corrosion cells (pits) during anodic and cathodic polarization would be the same[9]. This discussion concluded with the analysis that localized corrosion at cathodic potentials could occur but that it was rare and would not cause serious problems[9].

A number of modelling and experimental studies, including the present one, have been conducted to study the possibility for the occurrence of pitting under high temperature conditions and repository environments. Modelling studies[10] of pit propagation in low carbon steel showed that pit depth propagation increased with the presence of inert or nonreactive pit walls. It has not been determined that sufficient pit depth and corrosion product accumulation would develop to produce this protective effect assumed in the model.

Modelling of pitting has been discussed[11], and pitting was related to galvanic corrosion with two distinct electrodes in contact where the pit dissolves rapidly and the rest of the metal is passive and dissolves slowly. The rates of electrochemical processes within the pit and on the surface must be known as well as how these rates are affected by solution composition, temperature, current path and other environmental factors. Most of this information is accessible experimentally.

Some studies have been conducted of corrosion behavior of carbon steels in tuff repository environments[12]. These studies indicated that American Iron and Steel Institute (AISI) 1020 and 1025 steels and ASTM A-36 steel did not suffer excessive corrosion in the tuff environment but that more data, increased testing times and studies of galvanic effects were needed.

Useful information for predicting long-term durability of materials may be obtained from objects found in archaeological explorations. One example of a recent study of this type is of Roman nails. The Roman nails have a composition similar to A-216 steel and have been buried for 2000 years in Inchtuthil, Pertshire, Scotland. The nails were unearthed and found to be heavily corroded with the remaining material being ferrite with only a small amount of pearlite near the edge[13]. There were areas of localized corrosion but the origin could not be determined due to the overall gross corrosion attack. Approximately 900 nails were found at the burial site, but it is not known whether there were more and some had disintegrated.

These Roman nails are mentioned since it may be useful in making projections for the future to consider materials which have existed for relatively long times and to study their modes of degradation.

Current Work

The present investigation applied conventional electrochemical techniques to study pitting susceptibility of ASTM A-27 60-30 steel, and procedures and results are discussed. Electrochemical measurements involving electrode potential versus time and also cyclic polarization curves indicated that pitting would not occur. Microscopic examination of corroded specimens indicated overall general uneven surface corrosion with some shallow local attack in the ferritic areas. Since the specimen never passivated, the localized attack was related to preferential surface sites, and not to the usual electrode potential difference and current densities for producing pits of unknown depth and damage. These results indicate that deep pits of unknown amounts of damage do not occur in this type of steel under the conditions of these tests. The overall general corrosion, thick surface films, and nonpassivating conditions resulted in limited and shallow localized attack.

MATERIAL AND METHODS

The ASTM A-27 grade 60-30 steel sheet material was obtained from the Pacific Northwest Laboratory. The composition of the steel is given in Table 1, and this composition falls within the ASTM specification[16] for the composition of this steel.

Table 1. Composition of A 27, ASTM Grade 60-30 Steel in Weight Percent

C	Mn	Si	P	S	Mo	Cr	Ni	Fe
0.245	0.69	0.59	0.016	0.018	0.04	0.43	0.20	Bal.

Specimens were cut with a diamond saw and some specimens were placed in permanent mounts for etching and photographing, and others were mounted in temporary mounts for polishing in preparation for corrosion testing. All specimens were ground through 300 to 600 grit SiC papers and then polished with 6 μm and 1 μm diamond paste and were given a final polish in 0.05 μm Al_2O_3. Ethanol was used as a wetting agent in the final polish since the steel corroded or etched when water was used for the polishing. After the polishing, the specimens were washed with alcohol to remove any polishing material or contaminants. Microscopic and visual examinations were made to assure that specimens were clean. Specimens were prepared immediately before testing or were stored in a desiccator for a few days. Specimens for microscopic study were etched with a mixture of 9 parts ethanol to 1 part nitric acid, washed, dried and then studied using the light microscope.

3

One of the testing solutions, the Grande Ronde No. 4 water, was prepared using previously established methods and compositions[14]. The composition of this water was based on ground water samples which previously were collected and analyzed. The pH was adjusted to a value of 9.75 using additions of either 0.10 M HCl or 0.10 M NaOH. Stock solutions are prepared and later diluted as needed for use. The compositions of the stock solutions are given in Tables 2 and 3. One liter of synthetic Grande Ronde No. 4 water is prepared by adding 25 ml of stock solution A and 25 ml of stock solution B to 900 ml water. After the pH is adjusted, water is added to bring the water level to 1 L. The pH was checked again and was always measured before and after each test. The water was placed in the testing flask and brought to a temperature of 95°C before inserting the specimen.

Table 2. Composition of Grande Ronde 4 Basic Stock Solution A

Compound	Amount (g)
$Na_2SiO_3.9H_2O$	18.2
Na_2CO_3	6.40
Na_2SO_4	0.239
NaF	1.76
NaOH (50 % solution)	23.0
Water	(Add water to bring volume to 1 liter.)

Table 3. Composition of Grande Ronde 4 Acid Stock Solution B

Compound	Amount (g)
KCl	1.05
$CaCl_2.2H_2O$	0.323
HCl	219 ml of 2.0 M HCl
Water	(Add water to bring volume to 1 liter.)

Anodic and cyclic polarization measurements were made on the specimens in the specified environments. The specimen was placed in the 95°C solution and left at open-circuit potential for fifteen minutes prior to making the polarization measurements. Some of the polarization measurements were made by applying a potential to the specimen at the rate of 0.01 V/15 s starting from the corrosion potential and cycling back to the corrosion potential or lower. Other polarization measurements were made at a rate of 0.05 V/s for applying the potential and starting at 300 mV negative to the corrosion potential and ending at 200 mV negative to the corrosion potential. All voltages are in reference to a saturated calomel electrode (S.C.E.).

Some tests were made in Grande Ronde No. 4 water containing a mixture of 75 percent basalt and 25 percent bentonite. The Cohassett Flow basalt

rock and Wyoming bentonite clay were supplied by the Brookhaven National Laboratory. The basalt rock had been collected as large pieces and had to be crushed. This was difficult because the rock was hard and also there was concern regarding contamination by the crushing device. The rock was crushed by a motorized steel rock crusher. Prior to crushing, the rock crusher was washed consecutively with water, acetone and alcohol. Visual examination of the crusher for damage and of the crushed rock for crusher debris indicated no apparent contamination of the crushed rock by the crusher. The basalt and bentonite mixture was added to fill one half of the testing flask. The solution and mixture were held at temperature for one hour prior to inserting the specimen and beginning the test.

Additional tests were carried out in simulated J-13 well water, a water that represents a type found at Yucca Mountain, Nevada. The J-13 water was prepared using the formula given in Table 4. This composition is based on that given previously[15], but it has been altered to be ten times the normal concentration to represent a concentration of ions that might occur over extended times of wetting and drying. The water is heated but not boiled for mixing, and is saturated with some of the chemicals as indicated by the undissolved particles in the container. The pH of this solution is 8.5.

Table 4. Composition of Simulated J-13 Water Used

Chemical Compound	Grams/4 Liters
$NaHCO_3$	6.585
KOH	0.282
$SiO_2 \cdot XH_2O$ (1.87 % H_2O)	2.486
$CaCl_2$	0.464
$CaSO_4$ (0.92 g $CaCO_3$ + 0.88 g H_2SO_4)	1.288
$Ca(NO_3)_2$	0.096
$Mg(NO_3)_2 \cdot 6H_2O$	0.512
MgF_2 (0.093 MgO + 0.193 HF - 48%)	0.144
$LiNO_3$	0.028
$Sr(NO_3)_2$	0.0048
$BaCl_2 \cdot 2H_2O$	0.0036
$Fe(NO_3)_3 \cdot 9H_2O$	0.0144
H_3PO_4 (85%)	0.0056
$Al(NO_3)_3 \cdot 9H_2O$	0.0278

RESULTS AND DISCUSSION

Results of this work showed that the A-27 steel corroded continuously and did not undergo passivation under the testing conditions used. Specimens showed effects of corrosion in distilled water and in laboratory air. Discussions of the lack of passivity and general corrosion behavior of this material follow the description of the microstructures of the A-27 steel.

Susceptibility to pitting can be determined for metals which passivate by using a stimulation test such as the test described in the ASTM F 746, Standard Test Method for Pitting or Crevice Corrosion of Surgical Implant Materials[17]. Even though the A-27 steel did not readily passivate, the stimulation test described in F746, that is used for measuring susceptibility to pitting, was applied. No pitting potential could be determined using this method.

Microstructures

Examples of the microstructure of an uncorroded specimen are shown at two different magnifications in the micrographs of Figures 1 and 2. This microstructure consists of areas of ferrite (labeled f) and pearlite (labeled p). After anodic polarization, the specimen surface becomes uneven and three dimensional in appearance due to the corrosion attack on the surface. The pearlite is attacked more severely than the ferrite, as shown in Figure 3. Pearlite consists of alternating layers of cementite, Fe_3C and ferrite. The cementite is cathodic to the ferrite, and this promotes enhanced attack of the ferrite contained in the pearlite. Areas of local attack that could be identified as pits, are shallow and crystallographic, but are not deep pits in the usual sense of the term. Figure 4 shows that these areas also are present after cathodic polarization.
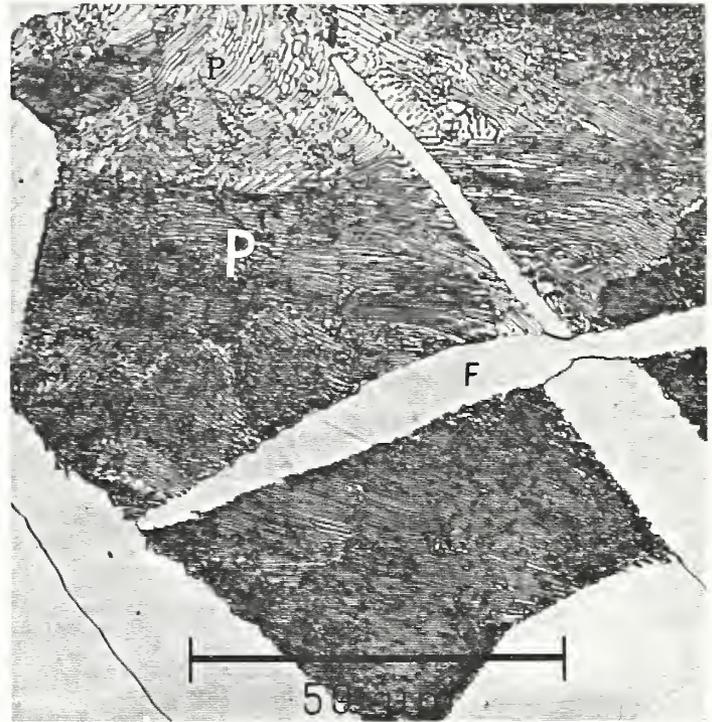
Figure 1. A-27 Steel, uncorroded
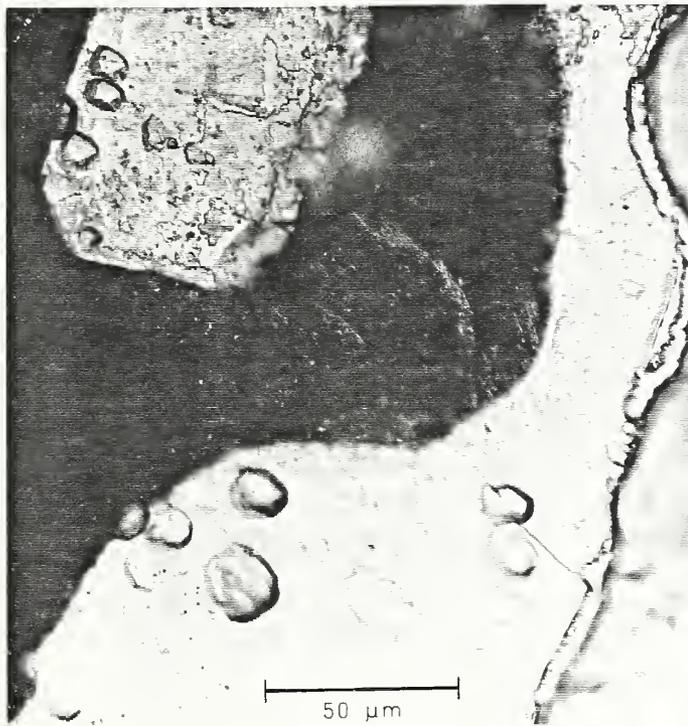

Figure 2. A-27 Steel, uncorroded

Figure 3. A-27 Steel, after anodic
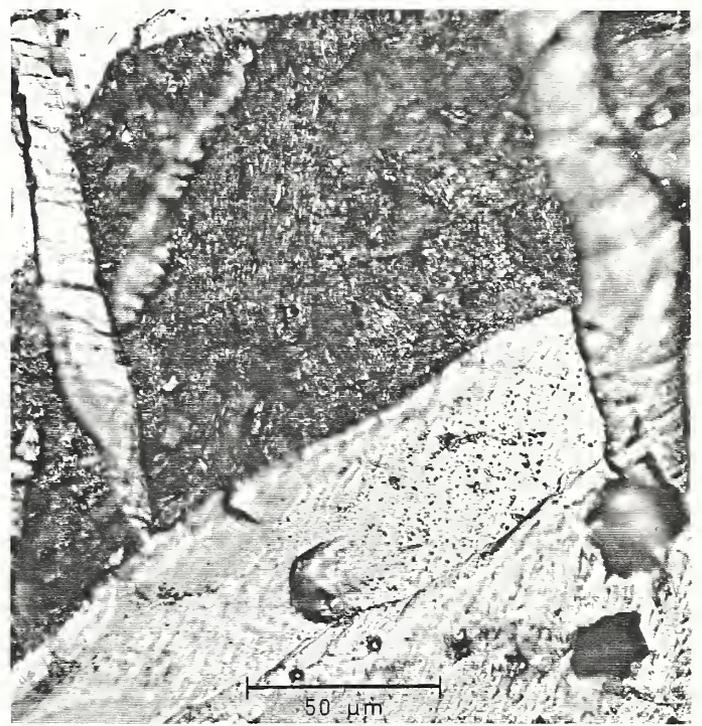   polarization

Figure 4. A-27 Steel, after
        cathodic polarization

7

Passivity

Upon immersion of the A-27 specimens in the test solutions, the electrode potentials decreased (in the direction of active corrosion) indicating continuous corrosion. Measurement of the open circuit potential versus time will show if one of the following reactions is occurring: (1) passivation -- the value of the potential rises in the noble direction, (2) pitting -- the values of the potential are erratic and (3) continuous corrosion -- the potential drops in the negative direction (less noble) and remains there. The A-27 steel is best described by continuous corrosion (case 3). Table 5 shows values of the open circuit potential of A-27 steel in Grande Ronde 4 water for a period of 18 hours. These values have become more negative after being in the solution for five minutes. There are some fluctuations in the potential, but the values remain around -0.600 V. The values of the potential varied depending on the condition of the metal surface that was placed in the solution but the trend, initially, toward more negative values during exposure was always the same.

Table 5. Open Circuit Potentials for A-27 Steel in GR-4 Water

Potential, (V) vs. SCE	Time, min.
-0.440	0
-0.600	5
-0.601	10
-0.649	20
-0.652	60
-0.627	120
-0.691	150
-0.602	18 hours

Other representative results of the initial open circuit potential and the potential after fifteen minutes are given in Table 6 for exposure in Grande Ronde No. 4 (GR-4) water (Test A) and for GR-4 water plus basalt and bentonite (Test B). Also given in this table are changes in the solution pH after testing.

As indicated by the open circuit potential for test A, the A-27 steel did not passivate in GR-4 water. The open circuit potential dropped from -0.46 V upon immersion to -0.59 V after fifteen minutes. This drop in potential occurred due to the absence of a passive film on the surface. The steel also did not passivate in GR-4 water plus basalt and bentonite as shown by the even lower potentials of -0.769 V initially and -0.787 V after 15 minutes.

Table 6. Open Circuit Potentials for A-27 Steel in Gr-4 Water with Basalt and Bentonite Along with Temperature and Initial pH_i and Final pH_f

Test	Time, min.	Media	pH_i	pH_f	Temp. C	Pot., V
A	0	GR-4 water	9.75		95	-0.46
A	15	GR-4 water	9.75		95	-0.59
A	After completion of test			9.2		
B	0	GR-4 water, ba-salt, bentonite	8.3		95	-0.769
B	15	GR-4 water, ba-salt, bentonite	8.3		95	-0.787
B	After completion of test			7.7		

Solution pH and Effects of Temperature and Basalt and Bentonite.

The initial pH (pH_i) of the GR-4 water was adjusted to 9.75 at 22°C, and decreased with the increasing temperature. The final pH (pH_f) of this water, at 60°C, after the anodic polarization test was 9.2. The pH of GR-4 water plus the basalt and bentonite was lower both at low and high temperatures. The pH of the GR-4 water was 9.75 at 22°C, and after combining 500 ml of this GR-4 water with 150 g of basalt and 50 g of bentonite, the pH_i of the mixture was 8.3 at 22°C. After completion of the anodic polarization measurements, the pH of this mixture at 60°C was 7.7.

Two readily observable effects of adding basalt and bentonite to the test media were the slurry formed in the test media and a lowering of the pH. The mixture of GR-4 water and basalt and bentonite was made and held at temperature approximately 1 hour prior to running the test. The crushed basalt provided a high surface area ratio/ unit Gr-4 water. It is possible that the chemistry of the environment containing this mixture could change over a longer period of time.

Polarization Measurements.

An example of a cyclic anodic polarization curve is shown in Figure 5 where the log of the current density is plotted versus the applied potential. These measurements were taken by starting at the corrosion potential. This is an example of the test labeled "A" in Table 6. Arrows on the curve indicate the direction of the applied potential during the test.

This curve shows that no passivation occurred and that the current density increased from the beginning. The current levels off somewhat at high currents at approximately 0.30 V due to the presence of a thick film which limits diffusion. Diffusion of the metal cations (outward) and of oxygen anions (inward) plus any other diffusion of electrons or lattice defects is necessary for the film to grow and to prevent polarization. Such thick films can offer some protection unless the films fall off. This film was observed to break up and fall off in some of the tests, causing sudden rises in the current.

In these tests represented by Figure 5, the reversal of the potential does not show a hysteresis in the current. The increased current in the remaining portion of the curve may be due to increased specimen area as a result of the corrosion during the test.

Figure 6 typifies a cyclic anodic polarization curve for the test represented by "B" in Table 6. In this test, measurements also were started from the corrosion potential. This curve starts from a lower corrosion potential when compared with that of Figure 5 and also shows that no passivation occurred. Here, as in the test of Figure 5, with increasing applied potential, the current becomes relatively constant at a potential of approximately 0.60 V due to the formation of a thick film and limited diffusion. The current, for the remaining portion of the curve, is different from that of Figure 5. It is lower. This may indicate increased protectiveness of the film or some reaction of the film with the basalt, bentonite and water mixture.

Figure 7 is a cyclic polarization curve for A-27 steel in Grand Ronde 4 water at 95°C and a pH of 9.75. These data were taken at a faster rate of applying the potential than that used for Figures 5 and 6, and measurements were started at -0.30 V less noble than the corrosion potential. The results of both sets of measurements are similar. There is no hysteresis in the beginning portion of this curve but the current remains high in the later portion of this curve. This hysteresis in the later portion may be due to the rate at which the potential was applied or it may be due to increased localized corrosion. The protection potential (indicated by E_p) and the final corrosion potential (indicated by E_{cf}) on the return curve, both are noble to the initial corrosion potential (indicated by E_{ci}). Data of this type should be used with care and effects of environmental and testing parameters should be carefully established.

Figure 8 is a cyclic polarization curve for A-27 steel in J-13 water at 95°C and a pH of 8.5. The initial corrosion potential, E_{ci} is more noble that the initial corrosion potential in the Grande Ronde 4 water, and the final corrosion potential is essentially the same. There is no hysteresis in the case of the J-13 exposure, and current on the return portion of the cycle remains lower than on the initial curve. The levels of Na^+ and Cl^- are less in the J-13 water, and the pH is lower than that of the Grande Ronde 4 water.
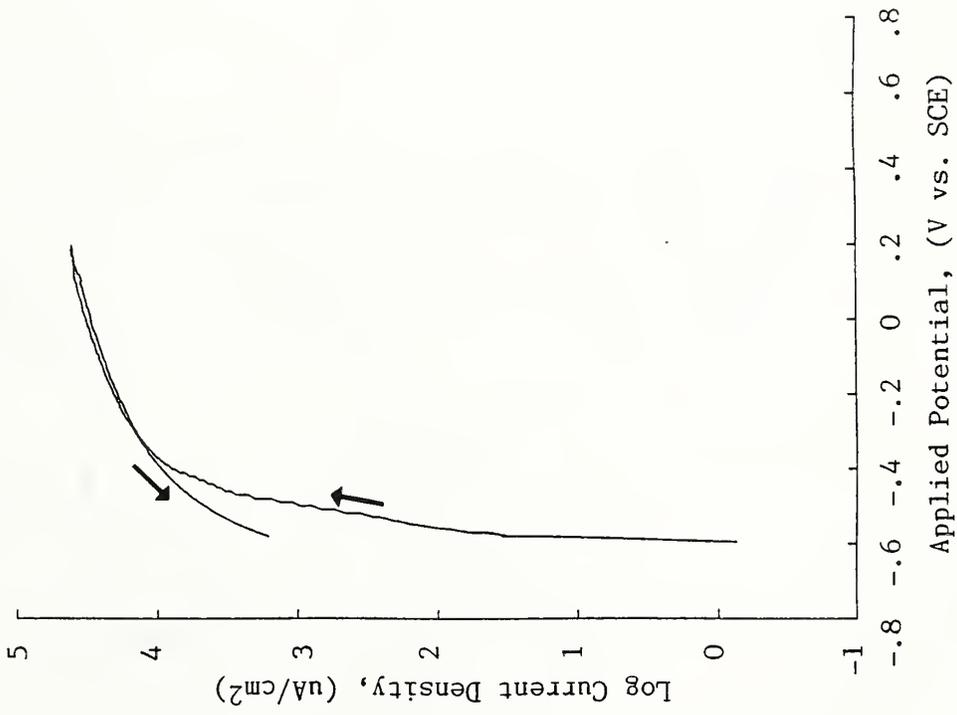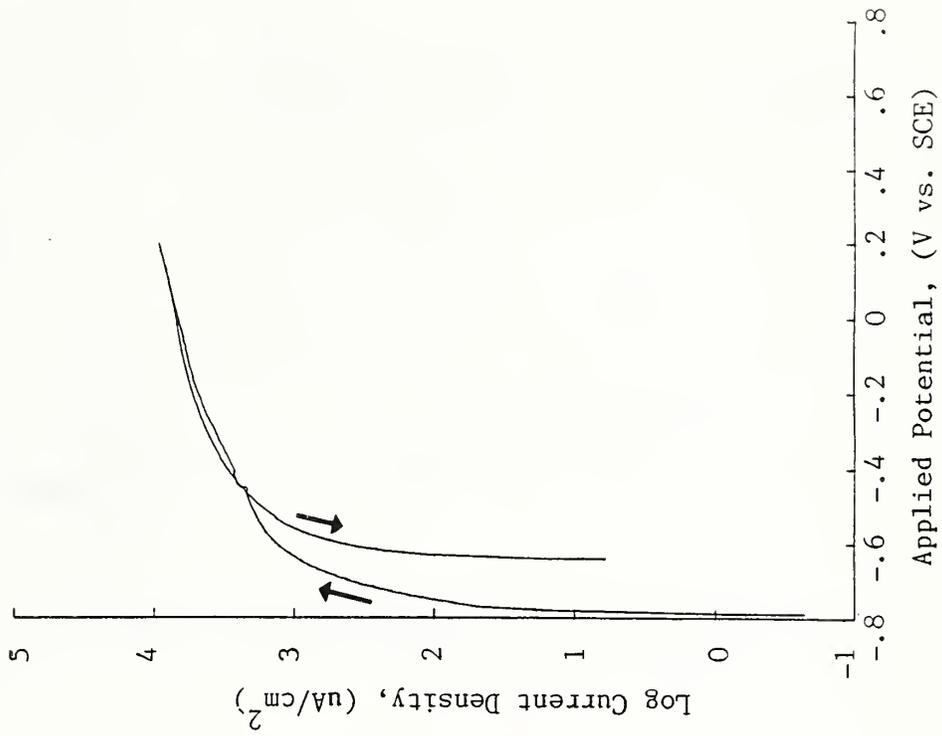
Figure 6. Anodic polarization curve; A-27 steel in 95°C GR-4 water with basalt and bentonite with a pH of 8.3

Figure 5. Anodic polarization curve; A-27 steel in 95°C GR-4 water with a pH of 9.75
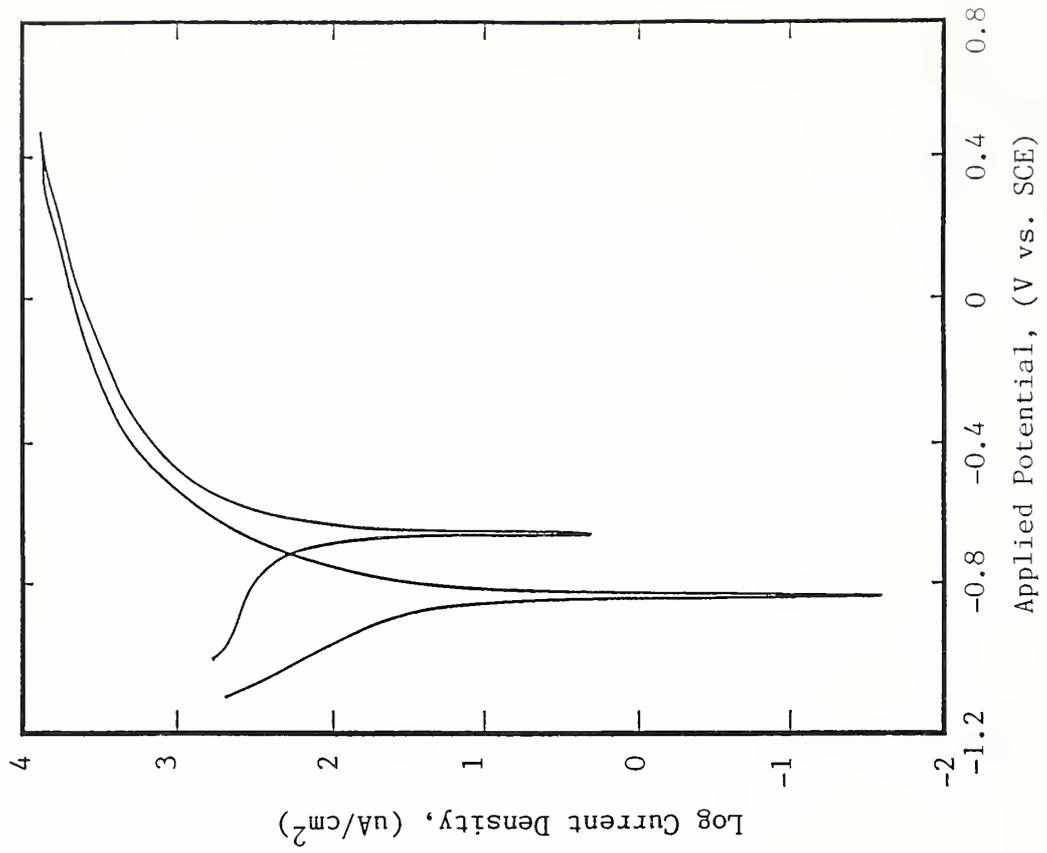
11

Figure 7. Cyclic polarization curve; A-27 steel in 95°C GR-4 water with a pH of 9.75
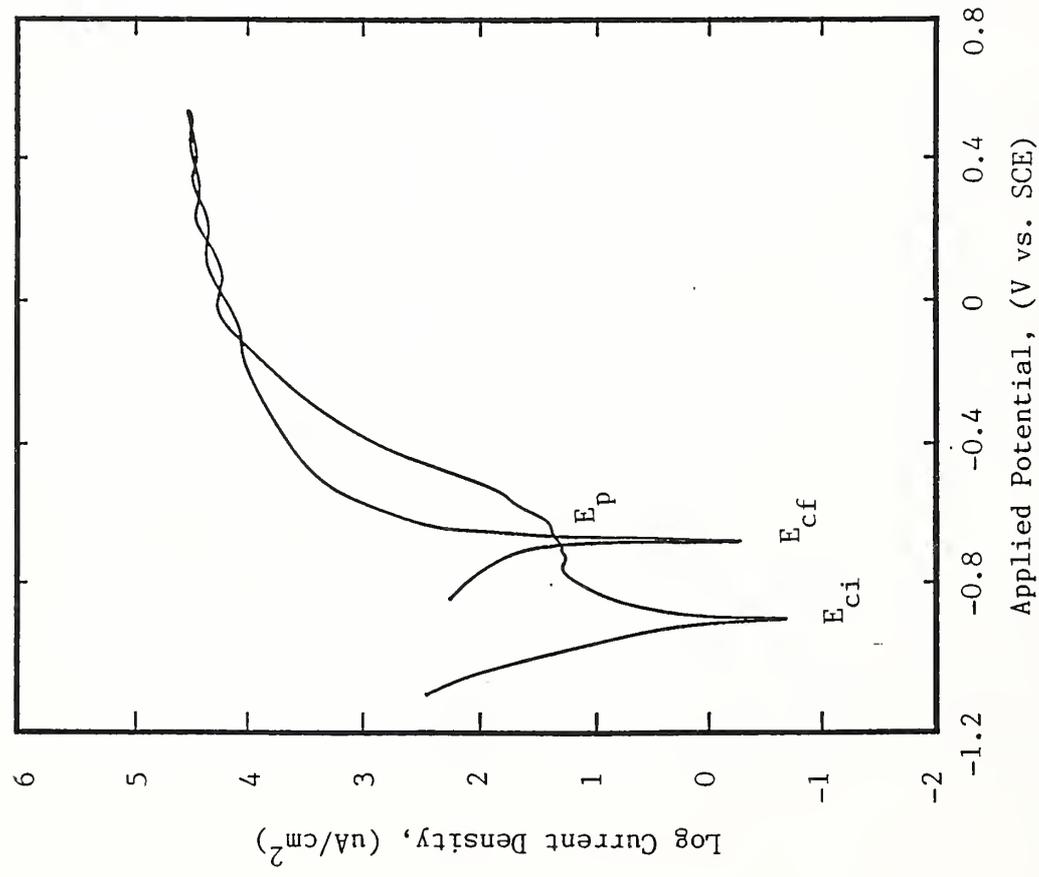
Figure 8. Cyclic polarization curve; A-27 steel in 95°C J-13 water with a pH of 8.5

12

Corrosion Rate Measurements

Measurement of the corrosion rate of A-27 steel in Grande Ronde 4 (GR-4) water and J-13 water are given in Table 7. Additional measurements were made in 3.5 percent NaCl, and these data are given in Table 8.

Table 7. Corrosion Rate Measurements in GR-4 and J-13 Water

	GR-4, 95°C, after 1 h	J-13, 22°C, after 1 h
E (I=0) (mV vs. SCE)	-604.88	-697.01
I Corr (uA/cm^2)	18.22	7.08
Corr Rate (mpy)*	8.41	3.35

Table 8. Corrosion Rate Measurements in 3.5 % NaCl at 22°C

	1h	4h	2 days	3days	4 days
E (I=0) (mV vs. SCE)	-570.4	-705.5	-745.9	-747.27	-767.65
I Corr (uA/cm^2)	25.32	3.72	2.84	2.64	3.26
Corr Rate (mpy)	11.82	1.73	1.33	1.23	1.52

Corrosion rates in the three different media, 3.5% NaCl water, GR-4 water and J-13 water are of the same order of magnitude but the rate is less in the J-13 water at the lower temperature. The corrosion rate decreases significantly over time as is shown in the case of NaCl in Table 7. It can be seen in the polarization curves, Figures 6 through 8, that the current levels off at a an electrode potential of approximately 0.3 V vs. a saturated calomel electrode (SCE).

SUMMARY

Anodic and cyclic polarization tests were conducted with A27 (ASTM grade 60-30) mild steel exposed in 95°C simulated Grande Ronde No. 4 water which had a solution pH ranging from 7.7 to 9.75, in J-13 water and in NaCl. The A-27 steel corrodes unevenly due to impurities and the presence of the cementite phase in the pearlite which is cathodic to the other phase, ferrite, in the pearlite. Corrosion rates decrease with time in this material and with increasing electrode potential due to the formation of a relatively thick surface film. The following conclusions can be made from this investigation.

1. Visible general corrosion occurs on A-27 ASTM grade 60-30 steel in laboratory air and in distilled water.

2. A-27 ASTM grade 60-30 steel does not passivate in simulated Grande Ronde No. 4 water under the conditions (times and temperatures) of this work and does not exhibit deep pitting corrosion.

3. Electrochemical electrode potential measurements showed that the open circuit potential decreased after immersion. This indicates that a passive film is not forming and that general (uniform) corrosion was occurring.

4. Localized attack was observed. The localized attack appeared to be crystallographic, and areas of localized corrosion were shallow. Theses areas of localized corrosion are not pits that meet the usual criteria for pits, because they are not the result of the local breakdown of a passive film. The exact cause of these features is not known.

5. Thick corrosion product films formed on the surface and occasionally, dropped off. Observation of surfaces under the films revealed an uneven and irregular morphology with preferential attack in the pearlitic regions (grains) of the A-27 steel.

6. Effects of adding basalt and bentonite to the simulated Grande Ronde No. 4 water were to produce a slurry type of mixture and to lower the pH. There may have been additional ions released into the mixture but this was not determined.

7. Increasing temperature lowers the pH of the simulated Grande Ronde No. 4 water.

Additional studies of mild steel in various media and for longer times would be useful for determining the materials durability. The irregular surface attack during the general corrosion should be more fully described as well as effects of varying amounts of pearlite in the microstructure, effects of varying ionic species and changing solution pH. The amount and distribution of impurity elements in the steel, such as Si, S and P, also should be considered.

REFERENCES

1. Kruger, J., Fundamental Aspects of the Corrosion of Metallic Implants, American Soc. for Testing and Materials Special Tec. Pub. 684, 107-127, 1979.

2. Syrett, B. C., PPR Curves - A New Method of Assessing Pitting Corrosion Resistance, Corrosion, Vol. 33, 6, 221, 1977.

3. Szklarska-Smialowska, Z., Pitting Corrosion of Metals, Nat. Assoc. of Corrosion Engineers, Houston, TX 77084, 1986.

4. Lumsden, J. B., Pitting Behavior of Low Carbon Steel, BWI-TS-014, August, 1985.

5. Westerman, R. E., Haberman, J. H., Pitman, S. G., Pulsipher, B. A. and Sigalla, L. A., Corrosion and Environmental-Mechanical Characterization of Iron/Base Nuclear Waste Package Structural Barrier Materials, PNL-5426, UC 70, 1986.

6. McCollough, I. S. and Scully, J., Pitting Attack on an Austenitic Stainless Steel in H_2SO_4, Corr. Sci., 707-709, 1969.

7. Ogura, Kotaro and Takesue, Noriyuki, Pit Formation in the Cathodic Polarization of Passive Iron, I. Dissolution of Passive Film and Pit Initiation, Corrosion, Vol. 36, (9), 487-490, 1980.

8. Ogura, K., and Ohama, T., Pit Formation in the Cathodic Polarization of Passive Iron, II. Effects of Ions, Corrosion, Vol. 37 (10), 569-574, 1981.

9. Ateya, B. and Pickering, H. W., Hydrogen in Metals, I. M. Bernstein and A. W. Thompson, Eds., Am. Soc. for Metals, Metals Park, OH, 207, 1974.

10. Beavers, John. A. and Markworth, Alan J., Pit Propagation of Carbon Steel in Groundwater, NRC Contract, B-0708, 1987.

11. Isaacs, H. S., Pitting Corrosion, U. S. NRC FIN A-3269, 1985.

12. McCright, R. Daniel and Weiss, Haskell, Corrosion Behavior of Carbon Steels Under Tuff Repository Environmental Conditions, Lawrence Livermore Lab., Mat. Res. Soc. Meeting, Boston, Nov., UCRL-90875, 1984.

13. Van Orden, A. C. and McNeill, M. B., Archaeological Artifacts Relevant to Long Term Corrosion Behavior, Proc. of the Mat. Res. Soc., Boston, MA, Dec., 1987.

14. Jones, T. E., Reference Material Chemistry - Synthetic Ground-Water Formulation, Rockwell International, Hanford WA, RHO-BW-ST-37 P, 1982.

15. Abraham, T., Jain, H. and Soo, P., Stress Corrosion Cracking Tests on High Level Waste Container Materials in Simulated Tuff Repository Environment, NUREG/CR-4619, BNL-NUREG-51996, p. 139.

16. A 27/A27M-87, Standard Specification for Steel Castings, Carbon, for General Application, American Society for Testing and Materials, Philadelphia, PA 191-1187, Vol. 01.02, 1-2, 1988.

17. F 746-87 Standard Test Method for Pitting or Crevice Corrosion of Metallic Surgical Implant Materials, American Society for Testing and Materials, Philadelphia, PA, 19103-1187, Vol. 13.01, 221-226, 1988.

ACKNOWLEDGEMENTS

U.S. DEPT. OF COMM. **BIBLIOGRAPHIC DATA** **SHEET** (See instructions)	1. PUBLICATION OR REPORT NO. NISTIR 89-4173	2. Performing Organ. Report No.	3. Publication Date SEPTEMBER 1989

4. TITLE AND SUBTITLE

Corrosion Behavior of Mild Steel in High pH Aqueous Media

5. AUTHOR(S)

Anna C. Fraker and Jonice S. Harris

6. PERFORMING ORGANIZATION (if joint or other than NBS, see instructions)

NATIONAL BUREAU OF STANDARDS
U.S. DEPARTMENT OF COMMERCE
GAITHERSBURG, MD 20899

7. Contract/Grant No.
FIN A-4171-9

8. Type of Report & Period Covered

9. SPONSORING ORGANIZATION NAME AND COMPLETE ADDRESS (Street, City, State, ZIP)

10. SUPPLEMENTARY NOTES

☐ Document describes a computer program; SF-185, FIPS Software Summary, is attached.

11. ABSTRACT (A 200-word or less factual summary of most significant information. If document includes a significant bibliography or literature survey, mention it here)

This paper reports on a study of the corrosion behavior and localized corrosion susceptibility of mild steel in a simulated ground water with a pH of 9.75 and at a temperature of 95°C. The steel used in the study was A27, ASTM Grade 60-30. This steel did not passivate in the aqueous environment used. The corrosion rate decreased with exposure time. Corrosion occurred in an uneven form over the surface, and although some pitting may have been present, no deep pits were observed. The amount and distribution of the areas of ferrite and pearlite as well as the impurities were determined to be important as related to uneven corrosion and to localized attack.

12. KEY WORDS (Six to twelve entries; alphabetical order; capitalize only proper names; and separate key words by semicolons)

A27 steel, steel, mild steel, corrosion, pitting, corrosion rate, aqueous corrosion

13. AVAILABILITY

[X] Unlimited

☐ For Official Distribution. Do Not Release to NTIS

☐ Order From Superintendent of Documents, U.S. Government Printing Office, Washington, D.C. 20402.

[XX] Order From National Technical Information Service (NTIS), Springfield, VA. 22161

14. NO. OF PRINTED PAGES
19

15. Price
A02